Extended data set for the equation of state of warm dense hydrogen isotopes

P. Loubeyre,[1] S. Brygoo,[1] J. Eggert,[2] P. M. Celliers,[2] D. K. Spaulding,[3] J. R. Rygg,[2] T. R. Boehly,[4]
G. W. Collins,[2] and R. Jeanloz[3]
[1]*CEA, DAM, DIF, F-91297 Arpajon, France*
[2]*Lawrence Livermore National Laboratory, Livermore, California 94551, USA*
[3]*University of California, Berkeley, California 94720, USA*
[4]*Laboratory for Laser Energetics, University of Rochester, Rochester, New York 14623, USA*
(Received 7 September 2011; revised manuscript received 15 October 2012; published 24 October 2012)

Laser-driven shock wave measurements on hydrogen and deuterium precompressed in diamond anvil cells from 0.16 to 1.6 GPa provide new shock Hugoniot data over a significantly broader range of density-temperature phase space than was previously achievable. Observations of shock velocity and thermal emission provide complete equation of state data (pressure, density, internal energy, and temperature) in the dense fluid regime up to 175 GPa. This data set is used to benchmark recent advanced *ab initio* calculations and is seen to be in good agreement with a maximum 8% density difference above 100 GPa. Thermodynamic quantities (specific heat and Gruneisen coefficient) are calculated directly from the data and compared to theory. Optical reflectivity data show a continuous transition from an electrically insulating to conducting fluid state and reveal that this transition is increasingly sensitive to temperature with increasing density. *Ab initio* calculations are observed to underestimate the temperature onset of metallization.

DOI: 10.1103/PhysRevB.86.144115 PACS number(s): 62.50.−p, 64.30.−t, 52.25.Kn

I. INTRODUCTION

Vigorous theoretical and experimental effort continues to be focused on understanding the properties of hydrogen at conditions where the Fermi energy, thermal energy, and Coulomb interaction energy are all comparable (specifically, at densities exceeding ∼0.1 mol H/cc and temperatures below 1 eV). Testing and validation of the equation of state (EoS) of hydrogen isotopes remain a critical issue for a variety of disciplines. Indeed, the relationship between pressure, density, energy, and temperature is essential for modeling the interior structure and evolution of astrophysical bodies (e.g., Jupiter and most known exoplanets)[1] as well as for inertial-confinement fusion (ICF) experimental design.[2,3] In addition, fundamental questions remain regarding the relation between metallization and dissociation,[4] the possible existence of a plasma phase transition,[5] and the importance of quantum nuclear effects.[6] Up to the present, the two most frequently used hydrogen EoS tables, SESAME[7] and SCVH,[8] have been based on the chemical approach. In both cases, free-energy models are used (including adjustments based on experiments) which are assumed to correctly describe the underlying atomic-scale physics of the molecular and plasma phases. The very limited experimental data available until now have made it difficult to quantify the accuracy of these approaches beyond a small region of phase space. Given the enormous advances in computational capacity in recent years, *ab initio* techniques can now be applied to the case of warm dense hydrogen. Such techniques have proven to be highly predictive for a number of systems, lending confidence to their application in the case of the EoS of hydrogen. These techniques may be validated against experimental data and because the underlying approximations vary little over the warm dense matter regime, their accuracy is expected to hold over a wide range of phase space. Grids of EoS data points have been generated over a large thermodynamic domain by several groups.[9–14] A thermodynamically consistent free-energy formulation of the hydrogen EoS was recently built based on a complete set of *ab initio* data.[14] It is the most advanced formulation of the EoS of hydrogen and a good representation of all these *ab initio* calculations. Differences of up to 50% in the compression ratio along the principle Hugoniot have been measured using different techniques, including gas gun,[15] magnetically driven flyer,[16] converging explosive,[17] and high-power lasers.[18–20] Discrepancies between data sets appear to be reduced by taking into account a revised EoS of quartz, used as a standard in many experiments.[21] Here, we set out to extend the thermodynamic domain of the experimental data set so as to benchmark the *ab initio* EoS more thoroughly and to provide a high level of confidence in the hydrogen EoS. The goals of this study are to confirm the determination of the principal Hugoniot of deuterium using a new approach, to extend measurements of the EoS of hydrogen off of the principal Hugoniot to cover a larger region of phase space, and to probe the transition from the molecular fluid to the plasma state with increasing density. To do this, we combine static and dynamic methods, generating laser-driven planar shock waves in precompressed samples of variable initial density. Quartz is used as the impedance-matching standard with its updated EoS.[21] Reflectivity measurements at the shock front are made to observe the transition to the conducting state. This paper is organized as follows: In Sec. II, details of the experimental method and diagnostics are presented; in Sec. III, an alternative determination of the principal Hugoniot of deuterium is made using the 0.3 GPa pre-compressed H_2 and D_2 samples; the complete data set is presented in Sec. IV; estimations of the heat capacity and the Gruneisen parameter are presented in Sec. V. In Sec. VI, the reflectivity data are presented and are compared to the results of quantum molecular dynamics simulations. Conclusions are presented in Sec. VII.

II. EXPERIMENTAL METHODS

A. Laser shock in precompressed targets

Our group has previously demonstrated the technique combining static and dynamic compression with laser-driven shocks on samples precompressed in the diamond anvil cell (DAC).[22,23] This technique has since been used to measure the properties of warm dense He.[24,25] Because the samples are confined by pressure, rather than cryogenically, the initial density of the H_2 and D_2 samples may precisely be controlled over a large range (in this case, from 0.7 ρ_{0L} to 1.9 ρ_{0L}, for pressures of 0.16 GPa and 1.6 GPa, respectively, where $\rho_{0L} =$ 0.084 mol H/cc is the D_2 cryo density). Variation of the initial density permits exploration of a set of Hugoniot curves for a given sample, hence exploration of phase space beyond the principle Hugoniot. Quartz is used as the impedance matching standard and as an *in situ* reference for relative measurements of reflectivity and temperature. The experimental configuration is shown in Fig. 1. The essential modification relative to a standard DAC is that the rear anvil, through which the shock front enters the sample, needs to be very thin to preserve the planarity and amplitude of the shock. 250-μm-thick diamond windows were used. The initial pressure of the precompressed targets was measured using the ruby fluorescence method (with an absolute precision of $\pm$0.03 GPa). The values of the energy and density of the initial state were obtained from piston-cylinder measurements of the fluid EoS of H_2 and D_2[26] (showing that the isotopic shift at 297 K is less than the initial pressure uncertainty). The preshot thicknesses of quartz and hydrogen were accurately determined by interferometry using the refractive indices of H_2[27] and quartz.[28] Laser energies of up to 6 kJ were delivered in a 1-ns temporally square pulse to produce shock waves that propagate through the diamond plate, the quartz pusher, and into the H_2 or D_2 samples. Shock velocity measurements with an accuracy of $\sim$1–2% were made in quartz and hydrogen using a velocity interferometer system for any reflector (VISAR).[29] The shocks were observed to be planar over at least a 400-μm width. Shock steadiness was quantified as a 3% velocity decrease during transit across the quartz pusher and hydrogen sample. Since both the quartz and the sample are transparent at the initial (precompressed) density, the velocity can be determined *in situ* as a function of time with the velocity at the quartz/hydrogen interface being used for determination of the hydrogen EoS by impedance matching. Shock reflectivity measurements were obtained at 532 nm using the VISAR signal. Temperatures of both shocked quartz and shocked hydrogen were inferred from a single-channel streaked optical pyrometer (SOP) centered at 650 nm. Metrology of the quartz and hydrogen target thickness was compared to the integrated shock travel time for consistency and is seen to agree to within 5%, i.e., the uncertainty of the preshot thickness determination.

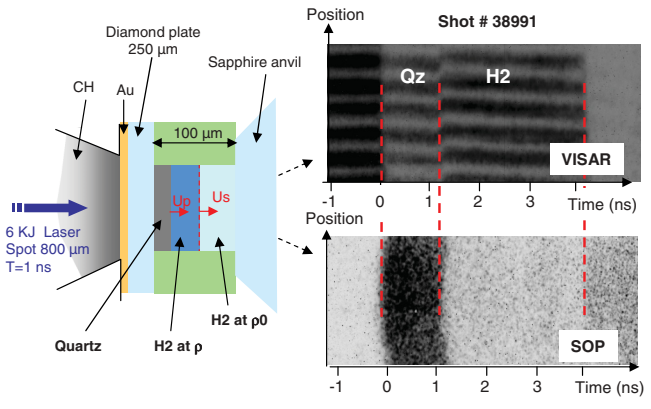

FIG. 1. (Color online) Experimental configuration for a laser shock in a precompressed target. A shock is driven from left to right by laser ablation of the CH layer. The velocity of the reflecting shock in quartz and in hydrogen is measured by a VISAR with a 532-nm probe beam. Temperature is extracted by the SOP from spectral radiance integrated over a band centered at 650 nm. Raw VISAR and SOP images show the spatial variation in the signal versus time.

B. The use of a quartz standard

The shock velocity in the hydrogen isotopes and the shock velocity in quartz are the two principle kinematic observables and are listed in Table I. When plotted against one another in Fig. 2, a shift with initial density is obtained in the case of D_2 whereas the points fall on the same curve in the case of H_2. However, it will be shown below that the pressure/compression Hugoniot data points fall on the same Hugoniot curve for both isotopes for a given initial density (for the same pressure at 297 K), as expected. Interestingly, since the shock pressure scales with the initial mass density, experiments on both H_2 and D_2 enable measurements over different regions of the Hugoniot curve: lower pressures for H_2 and higher pressures for D_2. Quartz is used as the standard for determination of the particle velocity in the hydrogen by impedance matching at the interface between the two materials.[24,30] Measurement of the shock velocity in the quartz provides the initial shock condition before it propagates into the hydrogen. As the wave reaches the interface, quartz undergoes isentropic release until its impedance matches that of shocked hydrogen. The impedance-matching technique requires knowledge of the Hugoniot and release behavior of quartz. Here we use the most recent determination of the Hugoniot of quartz in the high pressure fluid regime, measured using the Z facility (Sandia National Laboratory) from 200 GPa to 1500 GPa.[21] Quartz release isentropes were calculated using the mirror reflection of the principal quartz Hugoniot in the *P*-Up plane and by applying a correction calculated using the Mie-Gruneisen formalism.[31] For strongly shocked quartz in the dense fluid regime, the Mie-Gruneisen parameter has been estimated to be nearly constant to 0.66 ± 0.1.[32] Precompression has a slight effect on the initial density of the quartz and thus on its Hugoniot. The density change is estimated from the quartz EoS[33] and the associated effect on the Hugoniot was calibrated as a shift in the Us-Up plane, $C(\rho_0) = 2.4198(\rho_0 - 2.65)$.[32] The correction is less than 1% in pressure and density for an initial pressure of 0.16 GPa and 1% and 3% in pressure and density, respectively, for an initial pressure of 1.6 GPa. A minimum shock velocity of 14 km/s in quartz is needed to produce sufficient reflectivity for a VISAR measurement. This sets a lower pressure limit for the data collected. Because conservation of mass, momentum, and energy are obeyed at the shock front, the pressure, density, and energy of the final state are then determined from the particle and shock velocities

TABLE I. Shock velocities associated with various shots listed by the shot number at the OMEGA facility. The two kinematic experimental observables, the shock velocity in quartz, Us_{qz}, and the shock velocity in H_2 or D_2, Us_{H2} (Us_{D2}), are given with the random error arising from measurement limitations. The measured initial pressure at 297 K, P_0, with an uncertainty of 0.03 GPa, determines the initial density, ρ_0, with its associated uncertainty (Ref. 26) given in parentheses, according to the H_2/D_2 fluid equation of state. In the lower part of the table, some shots have no value for the shock velocity in H_2 or D_2 because due to some problem in the VISAR measurement it could only be inferred from transit time, hence with large error bars. However, the reflectivity and temperature measurements for these shots have been exploited.

H_2 Units	P_0 (GPa)	$\rho_0 \times 10^{-4}$ (g/cc)	Us_{qz} (km/s)	Us_{H2} (km/s)	D_2	P_0 (GPa)	$\rho_0 \times 10^{-4}$ (g/cc)	Us_{qz} (km/s)	Us_{D2} (km/s)
34834	0.31 (0.03)	881 (36)	20.5 (0.3)	28.6 (0.4)	40133	0.28 (0.03)	1705 (79)	21.9 (0.3)	30.1 (0.3)
34835	0.22 (0.03)	754 (46)	15.5 (0.3)	20.6 (0.4)	41449	0.3 (0.03)	1758 (75)	20.9 (0.3)	27.3 (0.3)
36174	0.7 (0.03)	1216 (19)	17.5 (0.3)	23.3 (0.5)	41459	0.27 (0.03)	1678 (81)	18.6 (0.3)	23.8 (0.3)
36176	0.74 (0.03)	1241 (18)	16.6 (0.4)	22.1 (0.3)	47715	1.2 (0.03)	2982 (25)	17.82 (0.3)	21.73 (0.3)
38326	0.13 (0.03)	576 (68)	24.1 (0.5)	35.1 (0.6)	47718	1.1 (0.03)	2895 (27)	22.34 (0.3)	28.67 (0.3)
38991	0.68 (0.03)	1204 (19)	21.5 (0.4)	30.1 (0.4)	47720	0.28 (0.03)	1705 (79)	20.85 (0.3)	27.8 (0.3)
38997	0.16 (0.03)	644 (59)	20.7 (0.5)	28.6 (0.5)	47721	0.16 (0.03)	1300 (120)	17.6 (0.3)	21.9 (0.3)
39000	1.48 (0.03)	1575 (10)	17.5 (0.6)	23.3 (0.5)	50369	0.58 (0.03)	2301 (44)	18.4 (0.24)	23.6 (0.31)
41451	1.44 (0.03)	1561 (11)	16.7 (0.7)	23.1 (0.4)	50370	1.3 (0.03)	3063 (23)	16.26 (0.28)	19.73 (0.29)
41458	0.16 (0.03)	644 (59)	16.3 (0.3)	21.6 (0.6)	50372	0.17 (0.03)	1342 (114)	20.98 (0.3)	27.6 (0.3)
43297	0.3 (0.03)	869 (37)	25.8 (0.3)	38.7 (0.3)	50378	1.51 (0.03)	3220 (21)	18.65 (0.53)	22.96 (0.65)
43298	1.37 (0.03)	1535 (11)	21.6 (1)	30.74 (0.6)	52253	1.51 (0.03)	3220 (21)	20.02 (0.23)	25.47 (0.28)
47716	0.16 (0.03)	644 (59)	19.3 (0.3)	26.3 (0.3)	53473	0.3 (0.03)	1758 (75)	21.3 (0.24)	28.62 (0.31)
47719	0.27 (0.03)	829 (40)	22.11 (0.3)	31.46 (0.3)	53474	1.71 (0.03)	3356 (19)	20.85 (0.54)	26.57 (0.65)
52250	0.32 (0.03)	893 (35)	20.28 (0.23)	28.09 (0.31)	53839	0.29 (0.03)	1732 (77)	22.73 (0.26)	31.12 (0.31)
53835	0.3 (0.03)	869 (37)	20.98 (0.54)	29.76 (0.71)	56360	1.46 (0.03)	3184 (22)	21.31 (0.3)	27.3 (0.3)
53838	0.16 (0.03)	644 (59)	23.46 (0.23)	33.81 (0.31)	56370	0.16 (0.03)	1300 (120)	21.3 (0.25)	28.4 (0.32)
55003	0.3 (0.03)	869 (37)	22.65 (0.54)	32.83 (0.72)	55005	0.17 (0.03)	1342 (114)	18.6 (0.6)	23.8 (0.39)
56366	1.47 (0.03)	1571 (10)	18.21 (0.25)	25.05 (0.35)	58084	0.16 (0.03)	1300 (120)	19.64 (0.2)	25.6 (0.2)
50377	0.3 (0.03)	869 (37)	22.69 (0.6)		47723	0.34 (0.03)	1857 (68)	19.9 (0.3)	
53471	0.16 (0.03)	644 (59)	18.31 (0.26)		50371	0.15 (0.03)	1256 (125)	12.5 (0.5)	
53472	0.3 (0.03)	869 (37)	17.92 (0.3)		50374	0.27 (0.03)	0.1678 (81)	11.3 (0.5)	
53478	0.33 (0.03)	905 (34)	20.9 (0.23)		50376	0.3 (0.03)	1758 (75)	12.9 (1)	
					50381	0.27 (0.03)	1678 (81)	19.2 (0.3)	

using the Rankine-Hugoniot equations.[34] Random errors were calculated within the impedance-matching construction using a Monte Carlo approach, propagating the uncertainty in the measurement of the shock velocities in quartz and hydrogen along with the uncertainty in the initial density. Systematic errors due to the uncertainty in the equation of state of quartz were also estimated by propagating the error in the Hugoniot, as given by the fit to the data from Knudson *et al.*[21] and

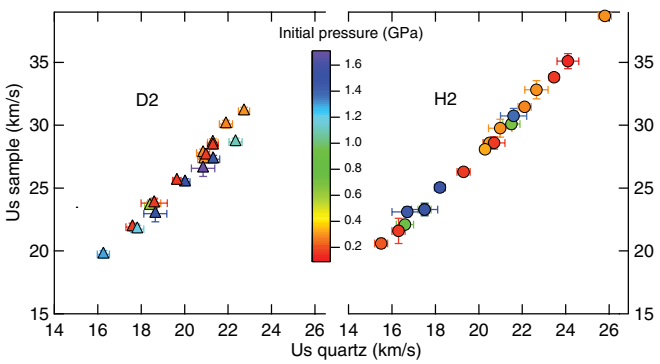

FIG. 2. (Color online) Evolution of the shock velocity in D_2 and H_2 versus the shock velocity in quartz. The triangles and dots represent D_2 and H_2 data, respectively. The color scale indicates the initial pressure in the target.

the error in the Gruneisen parameter, $\gamma = 0.66 \pm 0.1$. This systematic error is, at most, 20% of the total error in density and is mainly due to the error in the Gruneisen parameter. Absolute reflectivity and temperature measurements are typically very challenging, though relative measurements can be made with good accuracy. Such measurements are achieved in our pre-compressed targets by using the shock front in quartz as a relative reflectivity and temperature reference.[25] Both quantities have been previously measured as a function of shock velocity.[35] This calibration was subsequently revised, with a more recent version presented in the supplementary material of Ref. 25. A correction due to the precompression of quartz must be taken into account. The temperature correction was estimated using either a SESAME equation of state or by applying the Gruneisen model. Both estimates agree very well. Since the reflectivity of shocked quartz is primarily temperature dependent, the correction to the reflectivity is thus predominantly associated with the temperature change on the Hugoniot for the determined initial density. These corrections amount to adjustments of less than 4% in temperature and to less than 12% for the reflectivity.

III. THE PRINCIPAL HUGONIOT REVISITED

Precompression of D_2 to 0.3 GPa at 297 K offers an alternative way of generating data along the principle Hugoniot

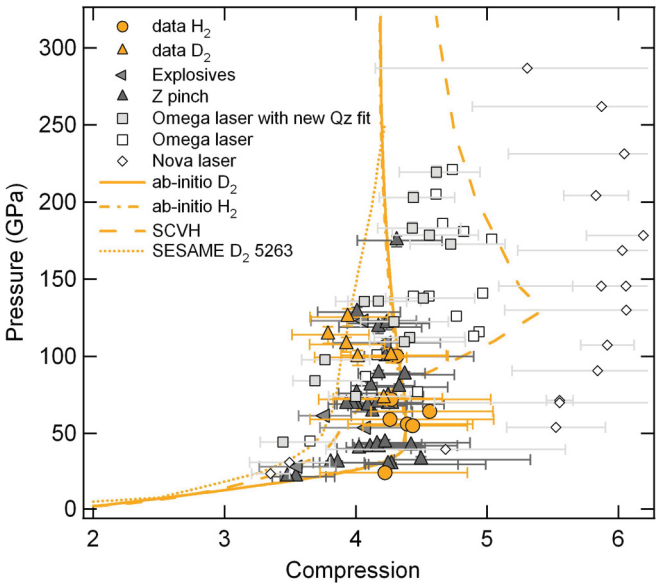

FIG. 3. (Color online) Pressure versus compression along the principal Hugoniot of deuterium. Shock data obtained from various platforms on cryogenic D_2 are represented by various symbols corresponding (respectively) to magnetic flyer (Ref. 16), explosives (Ref. 17), and laser shock (Refs. 18,19). The reanalzed data from Hicks *et al.* are included, using the updated quartz EoS. The present data obtained for D_2 (and H_2) at the same molar initial density, 0.084 mol H/cc, i.e., at 0.3 GPa at 297 K, are plotted respectively as solid yellow triangles and solid yellow circles. The experimental data are compared to various EoS models including SESAME (Ref. 7), SCVH (Ref. 8), and the *ab initio* model (Ref. 14). The *ab initio* EoS gives a very small isotopic difference between the D_2 and H_2 Hugoniots for the same initial density (solid and dotted lines, respectively).

since the initial molar density is the same as that of a cyrogenic sample at this pressure. Similarly, because an H_2 sample at 0.3 GPa precompression has an almost identical molar volume, its associated Hugoniot points are expected to fall on the same curve. To within the error bars, this is what we observe (Fig. 3). The present 0.3 GPa Hugoniot data points are also compared to prior studies on cryogenic D_2 targets and using different experimental platforms, including magnetically accelerated flyer experiments,[16] converging explosives,[17] and laser-driven shocks.[18,19] Most of these measurements are based on impedance-matching techniques using an aluminium standard in the case of the magnetic-flyer and converging explosive compression and quartz in the case of the OMEGA laser-driven compression data. In Fig. 3, the laser-shock data points of Hicks *et al.*[19] were reanalyzed using the updated quartz EoS adopted in the present study. A similar correction was proposed earlier by Knudson *et al.*[21] It can be seen that most of the data points are in agreement within their error bars with the exception of the laser-shock data from the NOVA platform which are systematically shifted to higher compression. This discrepancy is puzzling since the NOVA experiments were the only ones which relied on an absolute measurement of shock and particle velocities by transverse radiography. It is now suspected, however, that the transverse radiography method might have been affected by the quality of the aluminum-hydrogen interface, potentially interfering with the radiographic inference of the particle velocity. The difference between impedance match measurements and the NOVA data suggests the reported uncertainties in compression are too small in the latter study. The present data for precompressed targets of D_2 and of H_2 at 0.3 GPa confirm the determination of the Hugoniot of cryogenic D_2. In addition, these results demonstrate that EoS data from laser-driven shocks in precompressed targets can be measured as accurately as similar data obtained using more tested platforms. In Fig. 3, the pressure versus compression data along the principal Hugoniot are compared to three calculations: that obtained using SESAME table 5263,[7] widely used for ICF hydrosimulations; that using the SCVH model,[8] often used for astrophysical modeling; and the Hugoniot calculated using *ab initio* methods by several groups.[9–11,14] The calculated *ab initio* Hugoniot is in good agreement with the experimental data. The SCVH model yields too high a compression above 100 GPa while the SESAME EoS yields too small a compression ratio below 100 GPa. A similar conclusion was reached recently using an approach that directly compares measured shock velocity and temperature to those calculated by the various models and that, hence, circumvent the uncertainty due to impedance matching.[36] The present temperature versus pressure data along the principal Hugoniot are plotted in Fig. 4. These are in good agreement with previous experimental determinations from NOVA[37] or Z[38] experiments. All three calculations, SCVH, SESAME, and *ab initio*, go through the experimental data points. The difference between these three models is much less in temperature than in compression.

Quantifying the accuracy of the *ab initio* EoS would require data with error bars roughly an order of magnitude smaller than what can be achieved on current experimental platforms. An alternative method is to extend the density range of the experimental data set to explore phase space significantly off of the principal Hugoniot in order to probe relative changes.

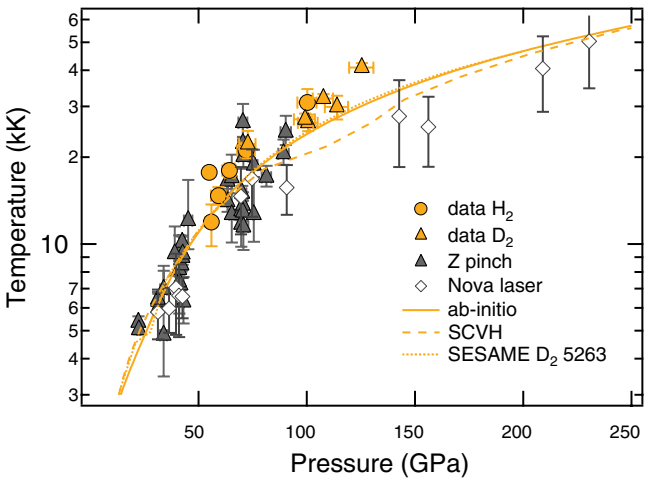

FIG. 4. (Color online) Temperature versus pressure along the principal Hugoniot of deuterium. The NOVA and Z data are from Ref. 37 and Ref. 38, respectively.

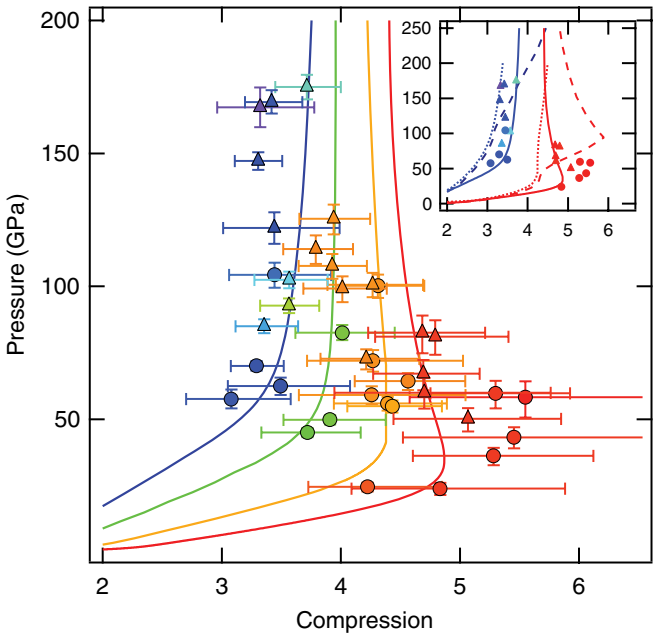

FIG. 5. (Color online) Pressure versus compression. Four initial precompressions of D_2 (H_2) samples at 297 K were studied: 0.16 GPa, 0.3 GPa, 0.7 GPa, and 1.6 GPa. The color scale and symbols are similar to Fig. 2. Error bars take into account random and systematic uncertainties. Inset: Only the Hugoniots at 0.16 GPa and 1.6 GPa are represented. Solid, dashed, and dotted lines are *ab initio* calculations (Ref. 14), SCVH (Ref. 8), and the SESAME (Ref. 7) EoSs, respectively.

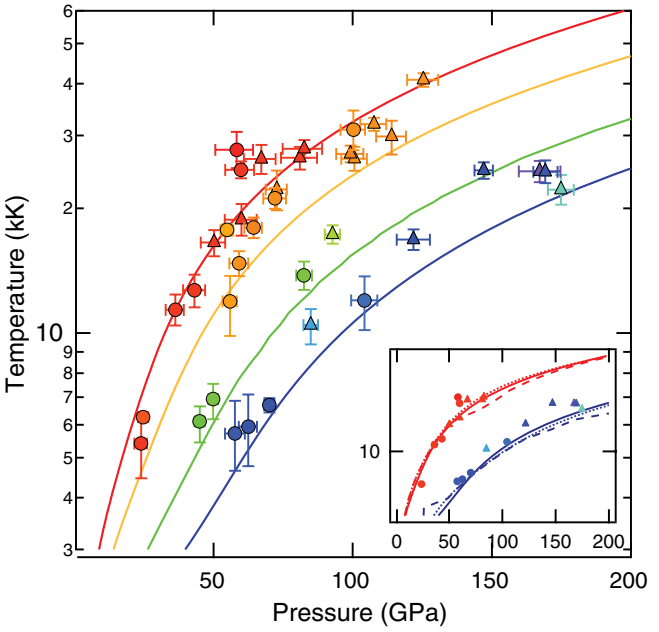

FIG. 6. (Color online) Temperature versus pressure. See Fig. 5 for labels.

IV. HUGONIOT DATA

Hugoniot data were collected for initial pre-compressions of 0.16 GPa, 0.3 GPa, 0.7 GPa, and 1.6 GPa. We thus cover a density range 2.7 times greater than previous investigations which were limited to the principle Hugoniot alone. The data are plotted in Fig. 5. The maximum compression along a given Hugoniot is observed to strongly decrease with increasing initial density, similar to what was observed in the case of helium.[24] This relative effect has little sensitivity to the systematic uncertainty in the quartz EoS and should thus act as a sensitive test of EoS models. Indeed, it is clear that the change in maximum compression is better reproduced by *ab initio* EoS than by the SCVH and the SESAME EoS (inset, Fig. 5). Figure 5 also demonstrates good agreement between experiment and the *ab initio* EoS for the 0.16 GPa Hugoniot, though the data points have much larger error bars than for samples at higher precompression. The errors are most pronounced for lowest precompression due to the increased uncertainty in the initial density caused by the ± 0.03 GPa error in the ruby pressure measurement prior to the shot as well as associated with release from the quartz into the hydrogen. Despite this, the fact that H_2 and D_2 fall on the same Hugoniot for a given precompression (as expected) is an indication that the impedance match construction with the present quartz EoS is quite satisfactory. Good agreement is also observed for the 0.3 GPa Hugoniot, although above 100 GPa the experimental data appear to show a slightly lower compressibility, yet within the error bars. This trend in compressibility is more apparent for the 1.6 GPa Hugoniot for which the error bars are smaller and the release of quartz for the impedance-matching construction better constrained. It is observed that the Hugoniot data have a density 8% smaller than the *ab initio* EoS. This deviation is of the same sign but slightly greater than the difference reported between the *ab initio* and the experimental solid EoS (for which 3% difference is seen[14]). This difference may be partly ascribed to the approximation for the GGA functional used in the *ab initio* calculations and possibly to dissociation, observed at higher temperatures than calculated, as shown in Sec. VI. The temperatures and pressures measured along the various Hugoniot curves are plotted against one another in Fig. 6. Again, the agreement is best for the *ab initio* EoS, though it is less a stringent test of the models than the compression curves since all calculations give similar results. The experimental data fall increasingly at higher temperature with increasing pressure. It implies that $(\delta P/\delta T)_{\rm exp} < (\delta P/\delta T)_{\rm cal}$. Since the conditions are roughly isochoric along the Hugoniot in the higher pressure region measured here, we can relate this slope to $(\delta P/\delta T)_V = \Gamma C_V/V = \alpha K_T$, where Γ, C_V, α, K_T are the Gruneisen parameter, the heat capacity at constant volume, the thermal expansion, and the isothermal compressibility, respectively. As shown below, the experimental Γ and C_V are respectively in good agreement and smaller than their *ab initio* values. Also, as shown above, the experimental compressibility is smaller than the *ab initio* value. The observed deviation at high pressure between experiment and the *ab initio* EoS in compression and in temperature versus pressure along the Hugoniots are thus consistent. Finally, it should be noted that the change in the initial density has a dramatic effect on the temperature along the Hugoniot. The complete data set is presented in Table II for hydrogen and Table III for deuterium.

V. THERMODYNAMIC ANALYSIS

Measurement of the shock and particle velocities permits determination of the variation in internal energy between the

TABLE II. H_2 Hugoniot data, pressure (P), compression ratio (ρ/ρ_0), and variation of internal energy, $E - E_0$, from impedance matching using a quartz reference and the shock velocity data given in Table I. The reflectivity, R, and the temperature, T, measured at the shock front are also given. For all quantities, the total errors (which include the systematic errors due to the quartz standard and random errors due to experiment) are given in parentheses. For the shots in the lower part of the table, the shock velocity in H_2 could only be obtained from transit time measurement hence not accurately enough for determining the compression ratio or the energy variation.

H_2	P (GPa) (−,+)	ρ/ρ_0 (−,+)	T (kK) (−,+)	R (−,+)	$E - E_0$ (kJ/mol H) (−,+)
34834	56 (3,2)	4.39 (0.47,0.5)	11.9 (2.1,1.8)	0.44 (0.09,0.13)	493 (31,29)
34835	25 (2,2)	4.22 (0.51,0.63)	6.3 (0.2,0.2)	0.13 (0.03,0.04)	252 (18,19)
36174	50 (2,2)	3.91 (0.4,0.47)	6.9 (0.7.0.6)	0.3 (0.08,0.12)	309 (13,12)
36176	45 (2,2)	3.72 (0.39,0.45)	6.1 (0.7,0.5)	0.18 (0.05,0.05)	270 (11,10)
38326	58 (8,6)	5.55 (0.99,1.25)	27.7 (2.7,2.9)	0.43 (0.06,0.06)	832 (88,107)
38991	83 (3,3)	4.01 (0.41,0.44)	13.8 (1.1,1.1)	0.42 (0.04,0.05)	519 (23,20)
38997	43 (4,4)	5.45 (0.95,1.36)	12.7 (1.2,1.1)	0.28 (0.07,0.07)	550 (50,56)
39000	63 (3,3)	3.49 (0.44,0.58)	5.9 (1.2,1.2)	0.26 (0.05,0.05)	290 (10,9)
41451	58 (4,4)	3.08 (0.38,0.5)	5.7 (1.1,1.1)	0.15 (0.04,0.05)	256 (9,8)
41458	24 (2,2)	4.83 (0.76,1.05)	5.4 (1,0.9)	0.03 (0.01,0.01)	297 (27,30)
43297	100 (5,4)	4.31 (0.37,0.39)	31 (3.4,3.5)	0.48 (0.12,0.13)	889 (54,53)
43298	104 (5,5)	3.44 (0.39,0.47)	12 (1.8,1.7)	0.53 (0.19,0.21)	488 (19,16)
47716	36 (4,3)	5.28 (0.71,0.84)	11.4 (1,1)	0.24 (0.05,0.07)	459 (42,47)
47719	64 (3,3)	4.56 (0.46,0.48)	18 (1,1)	0.47 (0.08,0.08)	609 (39,40)
52250	55 (2,2)	4.43 (0.41,0.42)	17.7 (0.6,0.6)	0.47 (0.05,0.06)	479 (29,27)
53835	59 (4,3)	4.26 (0.62,0.79)	14.7 (1,1)	0.39 (0.06,0.06)	524 (32,31)
53838	60 (6,5)	5.3 (0.57,0.63)	24.8 (1.2,1.2)	0.37 (0.05,0.06)	756 (69,77)
55003	72 (4,4)	4.27 (0.57,0.76)	21.1 (1.2,1.3)	0.46 (0.06,0.06)	637 (40,38)
56366	70 (2,2)	3.29 (0.22,0.23)	6.7 (0.3,0.3)	0.3 (0.06,0.08)	317 (11,10)
50377	70 (4,4)		19.4 (1.4,1.3)	0.5 (0.08,0.1)	
53471	33 (3,3)		9.1 (0.6,0.6)	0.18 (0.02,0.02)	
53472	38 (2,2)		8.1 (0.4,0.3)	0.17 (0.03,0.03)	
53478	62 (3,3)		14.5 (1,1.1)	0.37 (0.06,0.06)	

initial and the shocked state using the Rankine Hugoniot equations. The internal energy as a function of temperature or of pressure may then be used to calculate two thermodynamic quantities in warm dense hydrogen, namely the heat capacity at constant volume and the Gruneisen parameter. Figure 7 shows pressure versus the variation of internal energy for the set of measured Hugoniot curves. The Gruneisen parameter is defined as $\Gamma = V(\delta P/\delta E)_V$. Since the density is nearly constant along a given Hugoniot, as seen in Fig. 5, the Gruneisen parameter can be directly related to the slope of the evolution of internal energy versus pressure. The Gruneisen parameter determined in this manner is plotted in the inset of Fig. 7 versus the mean density of the data points along each Hugoniot. In Fig. 7, the (P, E) data points are also compared to the *ab initio* EoS,[14] showing very good agreement.

The variation of internal energy is plotted versus temperature for all the measured Hugoniot data points in Fig. 8. The data merge into a density-independent curve within the error bars. This indicates that the heat capacity at constant volume, $C_V = (\delta V/\delta T)_V$, is almost independent of density in this thermodynamical domain. A linear fit to these data above 10 kK, i.e., in the fully dissociated fluid, gives a value of 1.7 k_B per H atom (where k_B is Boltzmann's constant) at 0.4 ± 0.1 mol H/cc. The heat capacity ought to display a peak where molecular dissociation is taking place (between 5 kK and 10 kK) though observation of such a maximum was not possible in the present study since the shock velocity in hydrogen can only be measured accurately above the regime where dissociation begins and where the shock front reflectivity exceeds a few %. The measured C_V is compared to the value estimated by the *ab initio* EoS in the inset of Fig. 8 for two densities, 0.32 mol H/cc and 0.52 mol H/cc. The peak is due to the molecular dissociation around 2 kK. In the

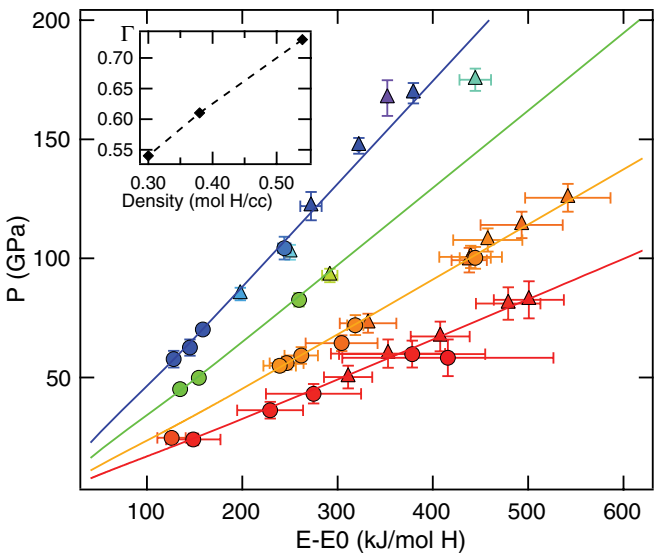

FIG. 7. (Color online) Pressure versus the variation of internal energy between the shocked state and the initial state. The color scale indicates the initial pressure of the sample and the different symbols, H_2 and D_2, as in Fig. 2. Inset: Gruneisen parameter versus mean density.

TABLE III. D_2 Hugoniot data, pressure (P), compression ratio (ρ/ρ_0), and variation of internal energy, $E - E_0$, from impedance matching using a quartz reference and the shock velocity data given in Table I. The reflectivity, R, and the temperature, T, measured at the shock front are also given. For all quantities, the total errors (which include the systematic errors due to the quartz standard and random errors due to experiment) are given in parentheses. For the shots in the lower part of the table, the shock velocity in D_2 could only be obtained from transit time measurement hence not accurately enough for determining the compression ratio or the energy variation.

D_2	P (GPa) (−,+)	ρ/ρ_0 (−,+)	T (kK) (−,+)	R (−,+)	$E - E_0$ (kJ/mol H) (−,+)
40133	114 (6,5)	3.79 (0.28,0.31)	29.9 (2.9,2.7)	0.38 (0.04,0.04)	493 (31,41)
41449	101 (5,4)	4.27 (0.39,0.42)	26.3 (1.7,1.8)	0.53 (0.13,0.15)	439 (26,34)
41459	73 (4,4)	4.21 (0.39,0.45)	22.2 (2.4,2.5)	0.57 (0.03,0.03)	332 (9,28)
47715	103 (3,3)	3.57 (0.3,0.32)		0.45 (0.13,0.16)	250 (17,8)
47718	175 (5,5)	3.71 (0.27,0.29)	22.2 (1.8,1.9)	0.48 (0.12,0.16)	444 (33,16)
47720	99 (5,5)	4.01 (0.33,0.37)	27.1 (1.3,1.3)	0.51 (0.1,0.11)	438 (36,37)
47721	50 (5,4)	5.07 (0.64,0.78)	16.5 (1.2,1.2)	0.33 (0.08,0.1)	311 (14,47)
50369	93 (3,3)	3.56 (0.25,0.26)	17.3 (0.9,0.9)	0.53 (0.07,0.08)	292 (6,14)
50370	85 (3,3)	3.35 (0.24,0.28)	10.5 (1,1.1)	0.38 (0.05,0.05)	198 (53,6)
50372	81 (7,6)	4.79 (0.52,0.61)	26.5 (1.7,1.7)	0.48 (0.05,0.05)	479 (9,67)
50378	122 (6,6)	3.44 (0.43,0.55)	16.8 (1,1)	0.58 (0.1,0.13)	272 (11,8)
52253	147 (3,3)	3.31 (0.2,0.2)	24.7 (1.2,1.2)	0.6 (0.05,0.05)	322 (33,10)
53473	108 (5,4)	3.93 (0.29,0.29)	31.9 (1.2,1.2)	0.51 (0.03,0.03)	458 (11,36)
53474	167 (8,7)	3.32 (0.36,0.46)	24.6 (1.5,1.6)	0.67 (0.07,0.07)	352 (40,11)
53839	125 (6,5)	3.94 (0.3,0.31)	40.9 (1.6,1.6)	0.52 (0.17,0.21)	542 (13,44)
56360	169 (4,4)	3.42 (0.23,0.26)	24.5 (1.5,1.6)	0.55 (0.05,0.05)	379 (58,12)
56370	83 (8,6)	4.68 (0.48,0.53)	27.8 (1.4,1.4)	0.34 (0.04,0.04)	501 (39,75)
55005	60 (6,5)	4.7 (0.76,1.06)	18.8 (1.6,1.7)	0.37 (0.04,0.04)	353 (47,49)
58084	67 (6,5)	4.69 (0.45,0.47)	26.3 (2.1,2.1)	0.48 (0.04,0.05)	408 (0,61)
47723	93 (4,4)		22.6 (1.6,1.7)	0.59 (0.11,0.14)	
50371	24 (3,3)		7 (0.5,0.5)	0 (0,0.44)	
50374	25 (2,2)		4.9 (0.3,0.3)	0 (0,0.28)	
50376	33 (4,4)		6.3 (0.8,0.8)	0.15 (0.07,0.12)	
50381	79 (4,4)		16.5 (0.9,1)	0.51 (0.11,0.17)	

following section, we will show that experimental dissociation takes place around 5 kK based on reflectivity measurements. However, in the fully dissociated regime above 10 kK, C_V is observed to be almost independent of density. In this regime, the experimental value falls slightly below that predicted by the *ab initio* model.

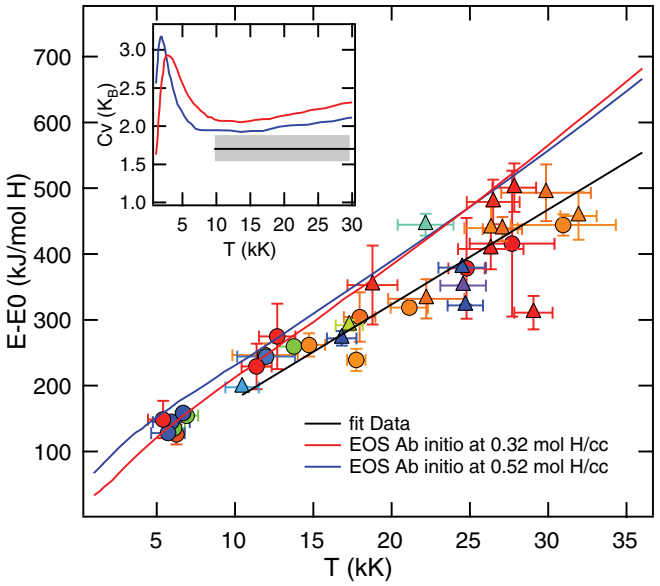

FIG. 8. (Color online) Variation of internal energy between shocked and initial states for H_2 and D_2 versus temperature. Color scale and symbols of the data points are identical to Fig. 2. Inset: C_V vs temperature. The gray region represents the error from the measurement.

VI. REFLECTIVITY MEASUREMENTS: INSULATOR TO CONDUCTING TRANSITION

Ab initio calculations of reflectivity[9,10,36] obtained using the Kubo-Greenwood formulation were previously compared with the NOVA laser reflectivity measurements as a function of pressure.[39] Good agreement was found, though this agreement may be diminished given that the NOVA pressures require a correction. It may be more insightful to consider the change in reflectivity versus temperature along the Hugoniot. *Ab initio* calculations have found that conductivity rises along the Hugoniot, closely following the dissociation of hydrogen molecules, and that the monomers then contribute substantially to the mobility of the electrons through the fluid. At a given density, dissociation is thus driven by an activation law, making temperature the most pertinent parameter. Also, although the present measurements are made relative to quartz, they are not dependent on the choice of quartz EoS and are thus free from any uncertainty therein. Reflectivity is plotted versus temperature in Fig. 9 for the various Hugoniots investigated here. A gradual increase in reflectivity is observed above about ∼5000 K, before reaching a plateau. The temperature onset of reflectivity (hence electrical conduction) appears weakly dependent on initial density; however, the rise in reflectivity with temperature steepens with molar density. The data are represented in Fig. 9,

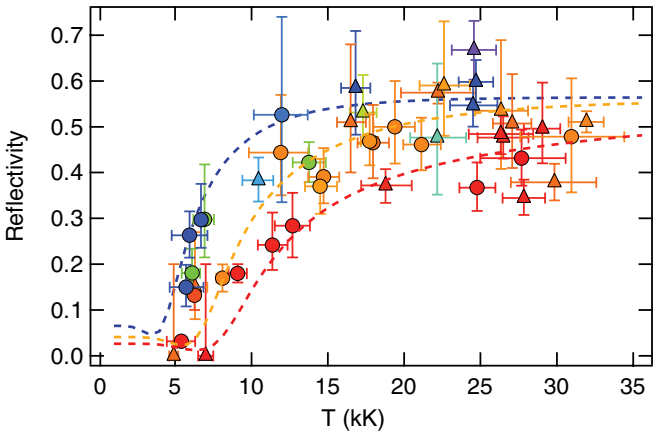

FIG. 9. (Color online) Change in reflectivity along the Hugoniots corresponding to different initial densities. The reflectivity is obtained from VISAR measurements at 532 nm. The color scale, as in Fig. 2, corresponds to the initial pressure. The dots and triangles represent H_2 and D_2 data, respectively. The colored dashed lines are physically constrained fits based on a Drude model using a Fermi-type dissociation fraction, as explained in the text.

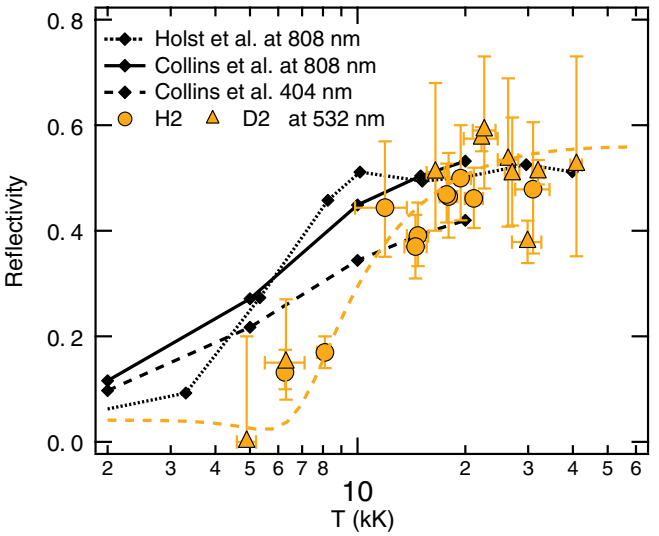

FIG. 10. (Color online) Reflectivity versus temperature along the principal Hugoniot. The black lines are the calculations of the reflectivity at 808 nm and 404 nm from Collins *et al.* (Ref. 9) and Holst *et al.* (Ref. 10). The yellow symbols and dashed line represent the experimental data at 532 nm and their fit.

along with a simple model for each Hugoniot (dashed lines) which provides some microscopic physical insight into the sample behavior. Namely, we used a Drude model for the optical conductivity, assuming the electronic density is directly proportional to the dissociation fraction and with the electron relaxation time given by the Ioffe-Regel limit.[25] This estimate of the relaxation time (4.8×10^{-17} s for a H plasma density of 1 mole/cc) is in very good agreement with the quantum Monte Carlo estimate[40] (4.9×10^{-17} s). The dissociation fractions, extracted along each Hugoniot, correspond roughly to the same density (see Tables II and III) and they are fitted to a Fermi-type function as suggested by the *ab initio* model.[14] This Fermi fit is then used along with the Drude model to calculate the reflectivity along the Hugoniot. Shown as dashed lines in Fig. 9, these calculated reflectivities are thus physically constrained and serve as much more than a simple guide to the eye.

To our knowledge, all quantum molecular dynamics calculations of the reflectivity versus temperature have been performed along the principal Hugoniot, corresponding to the 0.3 GPa Hugoniot here. Two calculations are compared in Fig. 10 with the experimental reflectivity along the 0.3 GPa Hugoniot. The calculation of Collins *et al.*[9] estimates the reflectivity versus temperature at 808 nm and 404 nm, whereas experimental measurements were performed at 532 nm. The calculation by Holst *et al.*[10] gives reflectivity vs pressure at 808 nm. This was converted to reflectivity versus temperature using the temperature-pressure relationship along the principle Hugoniot by the same group.[41] A slight difference is seen between the two calculations due to improved convergence and treatment of the zero point energy in the calculation by Holst *et al.*[10] In particular, the onset of reflectivity is given at approximately 2 kK in Collins's calculation and 3 kK in that by Holst *et al.* The experimentally measured onset of reflectivity is above 5 kK. That difference is much larger than the frequency shift in going from 808 nm to 532 nm. The underestimation of the onset temperature for reflectivity, hence conduction, is analogous to the underestimation of the electronic energy gap of solid hydrogen by density-functional theory (DFT).[42] The well-known DFT band gap problem at zero temperature is thus still present here although it was expected to be significantly reduced at high temperature.[43]

VII. CONCLUSION

In summary, the use of precompressed diamond-anvil cell targets for laser-driven shock experiments has enabled EoS measurements of warm dense hydrogen and deuterium significantly off of the principal Hugoniot. This data set has been used to benchmark the most advanced formulation of the hydrogen EoS based on *ab initio* calculations. This work provides an estimate of the level of confidence in the hydrogen EoS, suggesting better than 8% uncertainty. The onset of conduction in dense fluid hydrogen has also been investigated by measurement of optical reflectivity. In the density range studied here, conduction is seen to be primarily temperature driven. The onset of conduction takes place experimentally at about twice the temperature predicted by *ab initio* calculations. The rise in reflectivity becomes more sensitive to temperature with increasing density. This could be an indication of a possible evolution to the plasma phase transition at higher densities. In the future, experiments on larger laser facilities will permit precompressions up to an order of magnitude higher, allowing measurements along Hugoniot curves that should cross the predicted PPT line,[5] thus providing a definitive test of this intriguing first-order phase transition.

ACKNOWLEDGMENTS

We thank the OMEGA operations staff for their invaluable assistance. We thank M. Millerioux (CEA) for sample support. We thank Marius Millot for helpful comments and careful reading of the manuscript. This work was carried out under the NLUF program of the OMEGA laser facility of LLE.

[1]D. Saumon and T. Guillot, Astrophys. J. **609**, 1170 (2004).
[2]S. X. Hu, B. Militzer, V. N. Goncharov, and S. S. Skupsky, Phys. Rev. Lett. **104**, 235003 (2010).
[3]L. Caillabet, B. Canaud, G. Salin, S. Mazevet, and P. Loubeyre, Phys. Rev. Lett. **107**, 115004 (2011).
[4]I. Tamblyn and S. Bonev, J. Chem. Phys. **132**, 134503 (2010).
[5]M. Morales, C. Pierleoni, E. Schwegler, and D. Ceperley, Proc. Natl. Acad. Sci. USA **107**, 12799 (2010).
[6]E. Babaev, A. Sudbo, and N. Ashcroft, Nature (London) **431**, 666 (2004).
[7]G. Kerley, Sandia National Laboratories, Technical Report N SAND 2003-3613 (unpublished).
[8]D. Saumon, G. Chabrier, and H. van Horn, Astrophys. J. Suppl. Ser. **99**, 713 (1995).
[9]L. A. Collins, S. R. Bickham, J. D. Kress, S. Mazevet, T. J. Lenosky, N. J. Troullier, and W. Windl, Phys. Rev. B **63**, 184110 (2001).
[10]B. Holst, R. Redmer, and M. P. Desjarlais, Phys. Rev. B **77**, 184201 (2008).
[11]S. A. Bonev, B. Militzer, and G. Galli, Phys. Rev. B **69**, 014101 (2004).
[12]V. Bezkrovniy, V. S. Filinov, D. Kremp, M. Bonitz, M. Schlanges, W. D. Kraeft, P. R. Levashov, and V. E. Fortov, Phys. Rev. E **70**, 057401 (2004).
[13]S. X. Hu, B. Militzer, V. N. Goncharov, and S. Skupsky, Phys. Rev. B **84**, 224109 (2011).
[14]L. Caillabet, S. Mazevet, and P. Loubeyre, Phys. Rev. B **83**, 094101 (2011).
[15]W. Nellis, A. Mitchell, M. van Thiel, and R. Trainor, J. Chem. Phys. **79**, 1480 (1983).
[16]M. D. Knudson, D. L. Hanson, J. E. Bailey, C. A. Hall, J. R. Asay, and C. Deeney, Phys. Rev. B **69**, 144209 (2004).
[17]G. V. Boriskov, A. I. Bykov, R. Ilkaev, V. D. Selemir, G. V. Simakov, R. F. Trunin, V. D. Urlin, A. N. Shuikin, and W. J. Nellis, Phys. Rev. B **71**, 092104 (2005).
[18]G. W. Collins, L. B. Da Silva, P. Celliers, D. M. Gold, M. F. Foord, R. J. Wallace, A. Ng, S. V. Weber, K. S. Budil, and R. Cauble, Science **281**, 1178 (1998).
[19]D. G. Hicks, T. R. Boehly, P. M. Celliers, J. H. Eggert, S. J. Moon, D. D. Meyerhofer, and G. W. Collins, Phys. Rev. B **79**, 014112 (2009).
[20]T. Sano, N. Ozaki, T. Sakaiya, K. Shigemori, M. Ikoma, T. Kimura, K. Miyanishi, T. Endo, A. Shiroshita, H. Takahashi, T. Jitsui, Y. Hori, Y. Hironaka, A. Iwamoto, T. Kadono, M. Nakai, T. Okuchi, K. Otani, K. Shimizu, T. Kondo, R. Kodama, and K. Mima, Phys. Rev. B **83**, 054117 (2011).
[21]M. D. Knudson and M. P. Desjarlais, Phys. Rev. Lett. **103**, 225501 (2009).
[22]P. Loubeyre, P. Celliers, D. Hicks, E. Henry, A. Dewaele, J. Pasley, J. Eggert, M. Koenig, F. Occelli, K. Lee, R. Jeanloz, D. Neely, A. Benuzzi-Mounaix, D. Bradley, M. Bastea, S. Moon, and G. Collins, High Press. Res. **24**, 25 (2004).
[23]R. Jeanloz, P. Celliers, G. Collins, J. Eggert, K. Lee, R. McWilliams, S. Brygoo, and P. Loubeyre, Proc. Natl. Acad. Sci. USA **104**, 9172 (2007).
[24]J. Eggert, S. Brygoo, P. Loubeyre, R. S. McWilliams, P. M. Celliers, D. G. Hicks, T. R. Boehly, R. Jeanloz, and G. W. Collins, Phys. Rev. Lett. **100**, 124503 (2008).
[25]P. M. Celliers, P. Loubeyre, J. H. Eggert, S. Brygoo, R. S. McWilliams, D. G. Hicks, T. R. Boehly, R. Jeanloz, and G. W. Collins, Phys. Rev. Lett. **104**, 184503 (2010).
[26]R. Mills, D. Liebenberg, and C. Bronson, J. Chem. Phys. **68**, 2663 (1978).
[27]A. Dewaele, J. Eggert, P. Loubeyre, and R. LeToullec, Phys. Rev. B **67**, 094112 (2003).
[28]K. Vedam, and T. Davis, J. Opt. Soc. Am. **57**, 1140 (1967).
[29]P. Celliers, D. Bradley, G. Collins, D. Hicks, T. Boehly, and W. Armstrong, Rev. Sci. Instrum. **75**, 4916 (2005).
[30]M. Barrios, D. Hicks, T. Boehly, D. Fratanduono, J. Eggert, P. Celliers, G. Collins, and D. Meyerhofer, Phys. Plasmas **17**, 056307 (2010).
[31]R. McQueen, Los Alamos National Laboratory Report LA-UR-60-1996 (1989; unpublished).
[32]S. Brygoo, Ph.D. thesis, Ecole Polytechnique, 2006.
[33]D.B. McWhan, J. Appl. Phys. **38**, 347 (1967).
[34]Y. Zel'dovich and Y. Raizer, *Physics of Shock Waves and High-Temperature Hydrodynamic Phenomena* (Dover Publications, New York, 1966).
[35]D. Hicks, T. Boehly, J. Eggert, J. Miller, P. Celliers, and G. Collins, Phys. Rev. Lett. **97**, 025502 (2006).
[36]K. Falk, S. Regan, J. Vorberger, M. Barrios, T. Boehly, D. Fratanduono, S. Glenzer, D. Hicks, S. Hu, C. Murphy, P. Radha, S. Rothman, A. Jephcoat, J. Wark, D. Gericke, and G. Gregori, High Energy Dens. Phys. **8**, 76 (2012).
[37]G. W. Collins, P. M. Celliers, L. B. Da Silva, R. Cauble, D. M. Gold, M. E. Foord, N. C. Holmes, B. A. Hammel, R. J. Wallace, and A. Ng, Phys. Rev. Lett. **87**, 165504 (2001).
[38]J. E. Bailey, M. D. Knudson, A. L. Carlson, G. S. Dunham, M. P. Desjarlais, D. L. Hanson, and J. R. Asay, Phys. Rev. B **78**, 144107 (2008).
[39]P. M. Celliers, G. W. Collins, L. B. Da Silva, D. M. Gold, R. Cauble, R. J. Wallace, M. E. Foord, and B. A. Hammel, Phys. Rev. Lett. **84**, 5564 (2000).
[40]F. Lin, M. A. Morales, K. T. Delaney, C. Pierleoni, R. M. Martin, and D. M. Ceperley, Phys. Rev. Lett. **103**, 256401 (2009).
[41]M. P. Desjarlais, Phys. Rev. B **68**, 064204 (2003).
[42]M. Stadele and R. M. Martin, Phys. Rev. Lett. **84**, 6070 (2000).
[43]S. V. Faleev, M. van Schilfgaarde, T. Kotani, F. Leonard, and M. P. Desjarlais, Phys. Rev. B **74**, 033101 (2006).